

Integration of untargeted metabolomics and network pharmacology for differential metabolites and potential physiological activities analysis of Huangjing Fu tea

Zhiqin Ma^{1,2}, Yang Meng², Pinzhi Zhang¹, Mengyuan Zhang¹, Bowen Gu^{1,2}, Puyu Zhang¹, Changqing Li^{3,4,5}, Chuanjing An^{3,4,5*}, Xiao Xiao^{6*}, Liehan Mi^{7*} and Yuefang Gao^{1,2*}

¹ College of Horticulture, Northwest A & F University, Yangling 712100, China

² Fu Tea Research and Development Centre, Northwest A & F University, Jingyang 713700, China

³ Hebei Sericulture Industry Technology Innovation Center, Chengde Medical University, Chengde 067000, China

⁴ Hebei Universities Characteristic Sericulture Application Technology Research and Development Center, Chengde Medical University, Chengde 067000, China

⁵ Sericultural Research Institute, Chengde Medical University, Chengde 067000, China

⁶ College of Biomass Science and Engineering, Sichuan University, Chengdu 610065, China

⁷ Shaanxi Traditional Chinese Medicine Hospital, Xi'an 710000, China

* Correspondence: anchuanjing@cdmc.edu.cn (An C); xiao_xiao@scu.edu.cn (Xiao X); 345756067@qq.com (Mi L); yuefanggao@nwafu.edu.cn (Gao Y)

Abstract

Huangjing (*Polygonatum sibiricum*) is a traditional Chinese medicinal herb, and Huangjing Fu tea (HJFT) is an innovative Fu tea (FT) product made of raw dark tea and Huangjing extract through the traditional 'flowering' technique. It not only enriches the flavor of FT but also promotes the development of functional tea beverages with potential health benefits. However, the metabolite profile and underlying physiological activities of HJFT remain unclear. Untargeted metabolomics was employed to compare the chemical compositions of FT and HJFT in this study. PCA and OPLS-DA indicated that a total of 49 differential metabolites were identified between FT and HJFT. These compounds predominantly belonged to the categories of lipid molecules, phenylpropanoids and polyketides, and organic oxides. KEGG pathway analysis revealed that these metabolites were mainly enriched in lipid metabolism absorption, substance synthesis, and hypoglycemic detoxification anti-inflammatory pathways. Besides, metabolite-target network analysis prediction of the 22 upregulated metabolites in HJFT suggested that DM15, DM2, DM17, and DM18 were the core compounds acting on multiple targets and signaling pathways. Furthermore, an integrated disease-target-metabolite network indicated that sterols and terpenoid derivatives, especially 6-deoxohomodolichosterone, might possess the most prominent potential efficacy in the management of type 2 diabetes mellitus (T2DM). This study revealed the comprehensive metabolism and network pharmacological characterization of HJFT, and highlighted its dual properties both as a daily beverage and a potential functional substance. These findings may offer a scientific foundation for the further development and commercialization of HJFT, and serve as a model for research on other dual-property functional beverages.

Citation: Ma Z, Meng Y, Zhang P, Zhang M, Gu B, et al. 2026. Integration of untargeted metabolomics and network pharmacology for differential metabolites and potential physiological activities analysis of Huangjing Fu tea. *Beverage Plant Research* 6: e024 <https://doi.org/10.48130/bpr-0026-0017>

Introduction

As a type of post-fermentation dark tea with a long history, Fu tea has become a research hotspot due to its special beneficial fungus, *Eurotium cristatum* (also called 'Golden Flower', 'Jin Hua' in Chinese), produced during the crucial process of 'flowering'^[1,2] and its associated health benefits. The 'flowering' process, also known as the 'golden flower' formation period, directly determines the unique flavor, quality, and health benefits of Fu tea. It takes approximately 10–15 d under controlled temperature (25–30 °C) and humidity (75%–85%) conditions for the golden-brown cleistothecia to grow inside the tea. During this process, the extracellular enzymes secreted by *E. cristatum* catalyze the oxidative polymerization of tea polyphenols^[1,2], reducing the content of astringent catechin components to mellow the taste of the tea. At the same time, many substances such as tea polyphenols, amino acids, carbohydrates, and cellulose, undergo complex transformations like oxidation, hydrolysis, and polymerization^[3]. As a result, cellulose is decomposed into soluble sugars, and amino acids react with carbohydrates, transforming into aromatic compounds^[4], enhancing the sweet taste of Fu tea. Rich bioactive secondary metabolites were

also produced, such as indole alkaloids and ferulic acid^[3]. These substances have distinct health benefits, including weight loss^[5], aiding digestion, lowering lipids, regulating blood sugar, improving gastrointestinal function, inhibiting cancer cell growth, and antioxidant effects^[6].

Huangjing (*Polygonatum sibiricum*), a traditional Chinese medicinal herb with both edible and medicinal values, contains multiple bioactive components, including steroidal saponins, polysaccharides, and flavonoids^[7,8]. It is known for its role in replenishing qi and nourishing yin, antioxidation and anti-aging activities, immunity modulation, and regulation of blood glucose and blood lipid levels^[8–12]. Recently, with the growing market of functional tea beverages^[13], blended products of Huangjing Fu tea have emerged^[14,15], which may enhance the health benefits through component interaction. Nevertheless, the bioactive components and the potential pharmacological effects during the 'flowering' process of HJFT remain unclear.

To systematically analyze different metabolite compounds between HJFT and FT, untargeted metabolomics was utilized to identify metabolites through database matching (e.g., HMDB), followed by bioinformatics analysis to screen out key differential

metabolites and reveal the metabolite pathways. Network pharmacology analysis was applied to construct multi-dimensional association networks to link metabolite targets with six disease targets, revealing the potential theoretical basis for predicting the effects of HJFT on metabolite profile and health. The findings indicated that in HJFT, lipids and organic oxide metabolites were increased, which may affect neurotransmitter receptor activity, the immune system, and vascular function through multi-target and multi-pathway interactions. Notably, a high coincidence was screened between gene targets associated with HJFT metabolites and T2DM, indicating the significant potential of HJFT in the prevention and treatment of diabetes. This study not only provides a theoretical basis for the functional properties of HJFT, but also offers guidance for the development of new functional tea beverages.

Materials and methods

Preparation of tea samples

Huangjing Fu tea (HJFT) and the control Fu tea (FT) were produced by Jingyang Fu tea Research and Development Center (Jingyang, Shaanxi Province, China). The Huangjing (*P. sibiricum*) used in the experiment was produced through a process of nine steaming and nine sun-drying methods^[16]. The raw dark tea used in this study was the first-grade samples from Shaanxi Province, China.

The preparation of HJFT is as follows. First, Huangjing was soaked in 50 °C water for 3 h to obtain the Huangjing water extraction. This extract was mixed to make raw dark tea, and the moisture content of the mixture was adjusted to 30%. Afterwards, the mixed material was steam-heated and piled up at 50–60 °C for 12 h, then pressed into tea bricks after re-steaming. When the tea bricks were cooled to room temperature, they were transferred to a flowering room at a temperature of 24–28 °C and relative humidity of 65%–85%. After 12–15 d, the interiors of the tea bricks were filled with cleistothecia of *E. cristatum*, indicating the completion of the flowering process. Subsequently, the tea bricks were gradually dried at increasing temperatures from 30 °C to 45 °C, and the final product, HJFT, was obtained.

As for the control sample FT, the same raw materials were processed in the same way as HJFT under the same conditions, except that pure water was added instead of the Huangjing extract to adjust the tea base moisture before the steaming step. The experiment was repeated three times and named HJFT1 to HJFT3, and FT1 to FT3, respectively.

Experimental method

Sensory evaluation

According to Chinese National Standard GB/T 23776—2018 Methodology for the sensory evaluation of tea, sensory evaluation was performed on the FT and the HJFT samples. Five-gram samples of tea were weighed and placed in evaluation cups, then infused with boiling water at 100 °C for 5 min. The tea infusion was subsequently poured into different evaluation bowls for assessment. Three key aroma components were identified, including baked, woody, and mushroom-like, as well as two key taste components, including mellow and thick, and smooth. A 10-point categorical scale was adopted to score the intensity of each aroma and taste attribute (0 = no perception, 5 = moderate perception, 10 = strong perception). The scores were calculated and visualized using a radar chart.

LC-MS analysis

Solid samples

Liquid Chromatography-Mass Spectrometry (LC-MS) was used to accurately identify and quantify metabolite components in HJFT and FT. Briefly, 500 μ L of 80% ice-cold methanol (LC-MS grade, Honeywell) was added to an Eppendorf tube with 50 mg of the samples, and mixed thoroughly. After incubation at –20 °C for 30 min, the extracts were centrifuged at 20,000 g for 15 min, and the supernatants were transferred into new tubes for freeze drying. The dried residues were redissolved with 100 μ L 80% methanol (LC-MS grade, Honeywell), and centrifuged at 20,000 g for 15 min again, then transferred to the sample bottles and stored at –80 °C. In addition, pooled QC samples were also prepared by combining 10 μ L aliquots from each extraction.

Liquid chromatography and mass spectrometry conditions

Thermo Scientific UltiMate 3000 HPLC ultra-high performance liquid chromatography (Thermo Fisher Scientific, Bremen, Germany), combined with Exactive high-resolution mass spectrometer (Thermo Scientific) were used for analysis. An ACQUITY UPLC T3 column (10 mm \times 2.1 mm, 1.8 μ m, Waters, UK) was used for chromatographic separation. The mobile phase consisted of A: Aqueous phase including 5 mmol/L ammonium acetate and 5 mm/L acetic acid, and B: Organic phase, LS-MS grade acetonitrile. The column temperature was maintained at 40 °C, and the flow rate was 0.3 mL/min with the following gradient: 0–0.5 min, 5% B; 0.5–7 min, 5%–100% B; 7–8 min, 100% B; 8–8.1 min, 100%–5% B; 8.1–10 min, 5% B.

The Q-Exactive detection was performed in both positive and negative ion modes for each sample. Precursor spectra (70–1,050 m/z) were collected at 70,000 resolutions to hit an AGC target of 3e6. The maximum injection time was set to 100 ms. Data-dependent acquisition (DDA) mode was used, and the top three most intense ions were selected for fragmentation. The fragment spectra were collected at 17,500 resolutions with an AGC target of 1e5 and a maximum injection time of 80 ms. In order to evaluate the stability of the LC-MS during the whole acquisition, a quality control (QC) sample (pool of all samples) was injected after every 10 experimental samples.

Metabolite identification

In order to facilitate the subsequent work, the results generated by LC-MS were optimized. Peak extraction and quality control were performed using XCMS2 software, and the extracted substances were annotated with sum formula ions using the CAMERA package. Quantification, identification, and statistical analysis of metabolites were performed using metaX software (v2.1.0), such as primary mass spectrometry information for database matching identification, and secondary mass spectrometry information matched with an in-house standard database for identification. The identified metabolites were annotated with metabolites using HMDB 5.0, KEGG 112.0, and other databases. At last, differential metabolites were filtered based on the thresholds of p value < 0.05 and VIP \geq 1 and FC > 2, or FC < 0.5, respectively. GO and KEGG enrichment analysis of differential metabolites was performed using Metascape (<http://metascape.org>)^[17]. Metware Cloud (<https://cloud.metware.cn>) was used to generate volcano plots, heatmaps, and OPLS-DA models.

Network pharmacology analysis

Network pharmacology analysis was used to further identify the active metabolites and predict the physiological activity effects of HJFT. The significantly upregulated compounds of the differential metabolites were selected as candidate active compounds. The putative targets of the compounds were predicted using PubChem

(<https://pubchem.ncbi.nlm.nih.gov>) and Swiss Target Prediction (www.swisstargetprediction.ch/index.php) (species set to 'Homo sapiens', probability > 0). GeneCards (www.genecards.org) (using the median relevance score as the cutoff) was used to predict disease targets. The network pharmacology was visualized using Cytoscape 3.10. Further, functional enrichment analysis of the targets was performed by GO biological process (BP), cell components (CC), molecular function (MF), and KEGG enrichment analysis using Metascape.

Statistical analysis

To intuitively and systematically present the data, Excel 2020 was used to process the data, including statistical processing such as threshold screening, metabolite classification statistics, and network pharmacological target statistics. Charts were drawn by Metware Cloud (<https://cloud.metware.cn>), Cytoscape3.10, and Photoshop.

Results and discussion

Sensory quality analysis

Sensory evaluation was conducted to investigate the flavor difference between FT and HJFT products. Changes in the soup color of the two samples are shown in Fig. 1a. Overall, no obvious variation

in color was observed. However, the soup color of HJFT was slightly more orange-yellow than that of FT. To systematically characterize the aroma profiles of FT and HJFT, three key aroma factors (baked, woody, and mushroom-like), and two key taste factors (mellow and thick, and smooth) were established based on sensory evaluation consensus, with their aroma intensities presented in the radar chart of Fig. 1b. FT was produced via traditional pile fermentation and flowering, resulting in a prominent mushroom-like aroma. In contrast, HJFT exhibited an intense baked aroma derived from the nine steaming and nine sun-drying processes of Huangjing. Although its mushroom-like aroma was retained, the intensity was reduced. As for the flavor, HJFT tasted mellow, thicker, and smoother than FT.

Characteristic components in FT and HJFT by LC-MS

PCA and OPLS-DA analysis

Untargeted metabolomics based on LC-MS was utilized to investigate the differential metabolites between FT and HJFT. Principal component analysis (PCA) was applied to the metabolite detection results of each tea group and the QC group. The first two principal components collectively explained 51.49% of the total variance, with PC1 and PC2 accounting for 33.69% and 17.80%, respectively (Fig. 2a). The PCA analysis plot revealed the separation between the

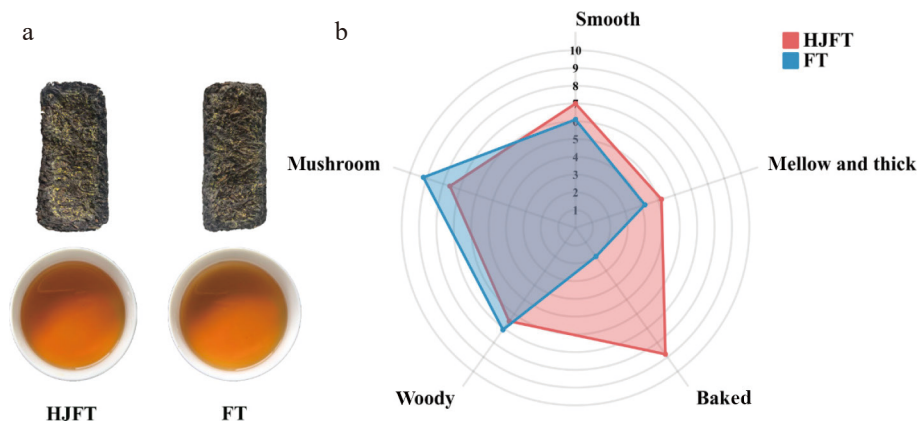


Fig. 1 Sensory evaluation correlation diagram. (a) FT and HJFT samples and the brewed tea infusion; (b) radar chart of FT and HJFT aroma intensity and taste characteristics.

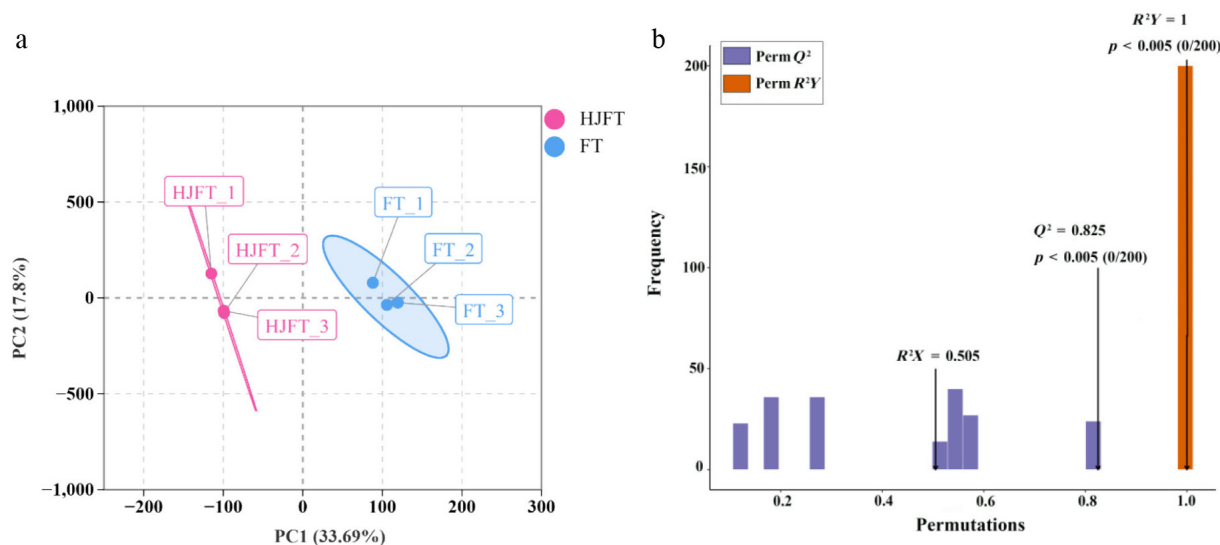


Fig. 2 PCA and OPLS-DA analysis. (a) PCA analysis plot; (b) OPLS-DA model of differential metabolites.

HJFT and FT groups, with minimal dispersion among the biological replicates. All biological replicates were within the 95% confidence ellipse, demonstrating the reliability of the experimental data and providing a foundation for subsequent screening.

OPLS-DA is a supervised discriminant analysis method that maximizes the differences between different groups, thereby better revealing the significant differences in the material components of FT and HJFT. In the OPLS-DA (Fig. 2b), $Q^2 = 0.825$, $p < 0.005$; $R^2Y = 1$, $p < 0.005$, conform to $Q^2 > 0.5$, $R^2Y > 0.5$ and $p < 0.05$, indicating a valid and predictive model. Collectively, the model demonstrates interpretability and acceptable predictability.

The major chemical components of FT and HJFT

To accurately identify the differential metabolites between FT and HJFT, untargeted metabolomics was employed. Among the initially identified metabolites, Class I was classified into 12 categories, predominantly including lipids and lipid-like molecules, phenylpropanoids and polyketides, organ heterocyclic compounds, benzenoids, organic acids and derivatives, and organic oxygen compounds. Class II was classified into 100 categories. The above-mentioned overall metabolites were screened based on the threshold (p value < 0.05 , VIP value ≥ 1 , and FC > 2 , or FC < 0.5), and 867 metabolites were identified. After excluding unclassified metabolites (unmatched secondary classification substances), 49 differential metabolites were obtained, with six categories of Class I (Fig. 3, inside ring) and 12 categories of Class II (Fig. 3, outside ring). Compared to FT, lipids increased during the flowering process of HJFT, among which glycolipid content showed a significant increase, while organic oxygen compounds exhibited a slight increase, which might be related to the presence of *Polygonatum sibiricum* polysaccharide (PSP)^[7,16]. Class I (inner circle) was classified in a broad and extensive manner, while Class II (outer circle) was further divided within the scope of Class I. To make a more precise and specific distinction of substances, Class II was selected as the main research object in the subsequent study.

Correlation analysis of differential metabolites

To identify the key differential components between HJFT and FT, metabolites were screened in both positive and negative ion modes

using thresholds, p value < 0.05 , VIP ≥ 1 , and FC > 2 , or FC < 0.5 . In the negative ion mode, a total of 25 differential metabolites were identified, including 24 upregulated metabolites and 1 downregulated metabolite. As in the positive ion mode, a total of 24 differential metabolites were determined, including 14 upregulated metabolites and 10 downregulated metabolites (Fig. 4a). The major components of differential metabolites were lipids and lipid-like molecules (including glycerophospholipids, glycerolipids, fatty acyls, prenol lipids, sterol lipids, sphingolipids), nucleosides, nucleotides and analogues, benzene and substituted derivatives, organic acids and their derivatives (such as carboxylic acids and derivatives), organic heterocyclic compounds (e.g., tetrapyrroles and derivatives, indoles and derivatives, pyridines and derivatives), and organic oxygen compounds (Fig. 4b). The detailed information of 49 differential metabolites of FT and HJFT were shown in Supplementary Table S1.

KEGG pathway enrichment analysis

To further elucidate the functional roles and pathways of the metabolites, 49 different metabolites were subjected to KEGG pathway enrichment analysis^[18] (Fig. 5). A total of 40 pathways covering 26 metabolites were identified, mainly associated with organismal systems, metabolism, human diseases, environmental information processing, and cellular processes. The key biological functions included lipid metabolism absorption, substance synthesis, hypoglycemic detoxification, and anti-inflammatory cellular immune responses. These pathways and biological enrichment analyses indicated that the upregulated compounds in HJFT could be involved in secondary metabolite synthesis, fragrance production, and various physiological activity functions.

Network pharmacology analysis of key metabolites in HJFT

Prediction of targets for active metabolites in HJFT

To further predict the physiological activities of HJFT metabolites and their potential involvement in related diseases, PubChem and Swiss Target Prediction were applied to predict the potential

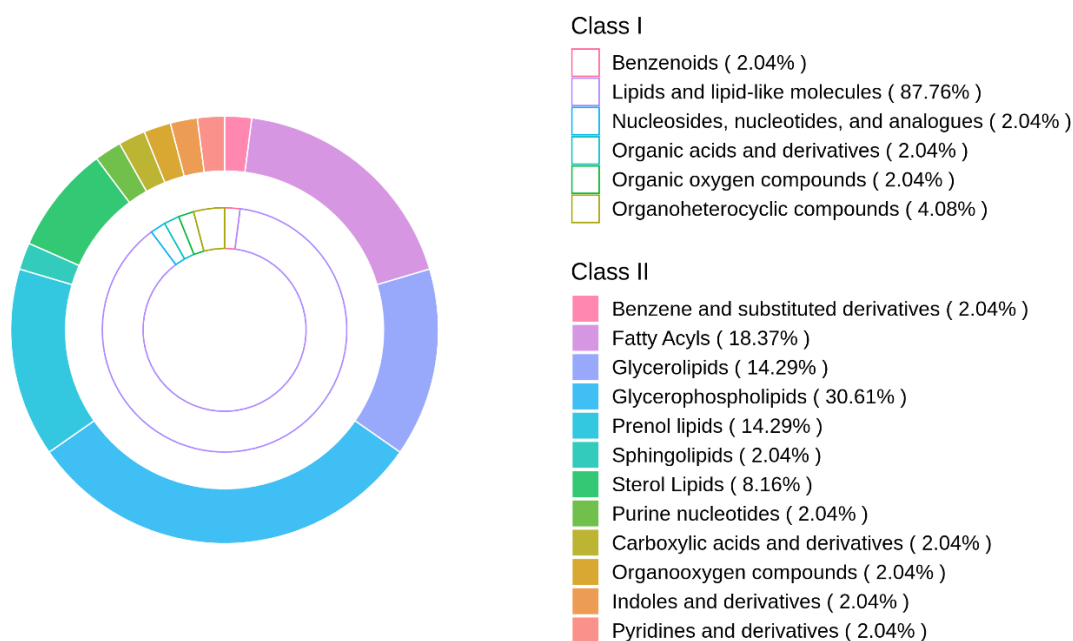


Fig. 3 Comparison of different metabolite classes in FT and HJFT. The proportion of Class I (inner circle) and Class II (outer circle) classifications based on the substances after screening.

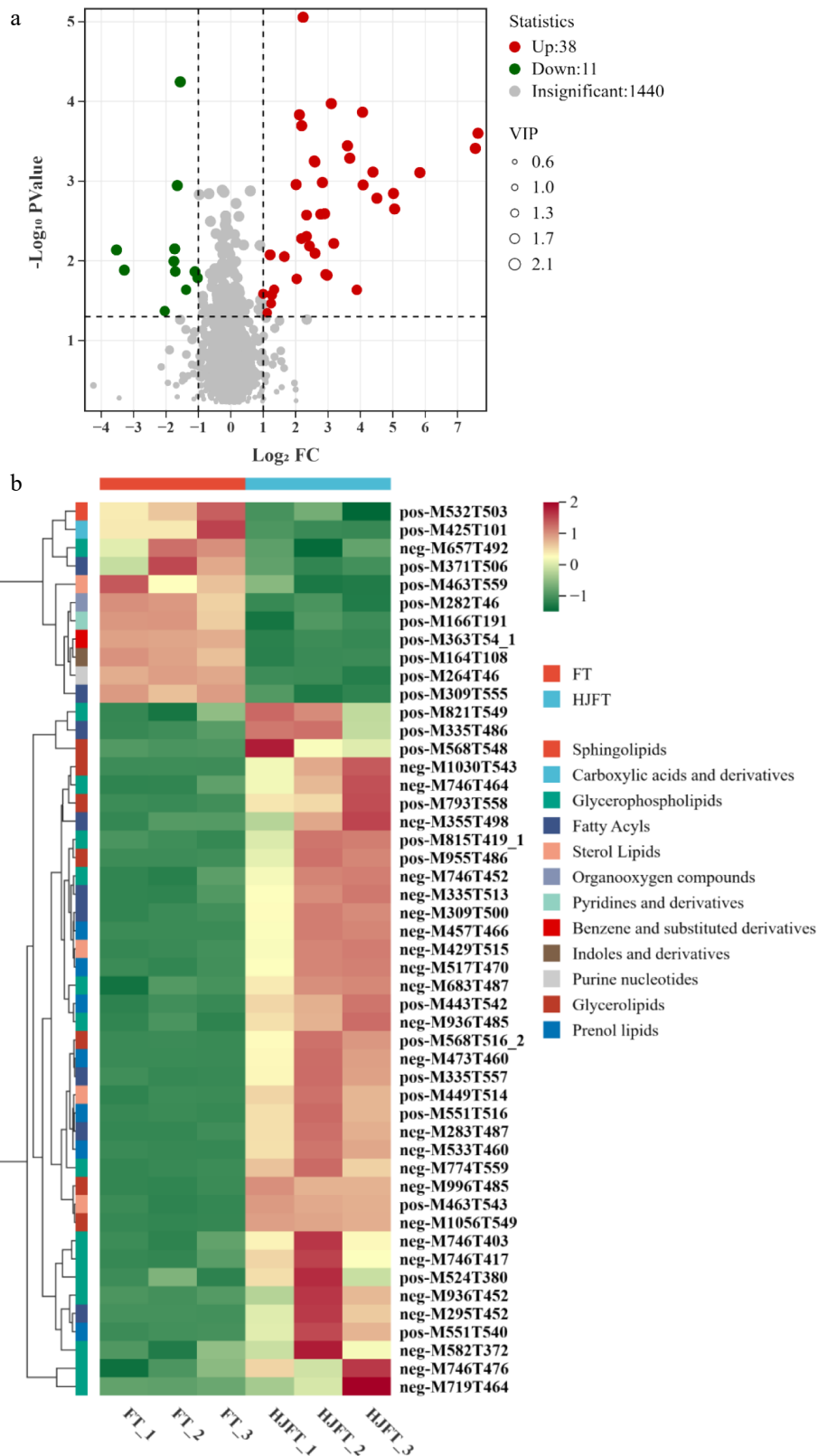


Fig. 4 Differential metabolites of FT and HJFT. (a) Volcano gram of upregulated and downregulated metabolites; (b) clustering heatmap of differential metabolites.

targets. Among the 38 upregulated metabolites, 16 compounds were excluded due to a lack of predicted targets, and the remaining 22 were listed in Table 1, with their metabolite-target network shown in Fig. 6. In this network, the red box represents the 22

metabolites, and the light blue diamond represents the target genes. These compounds could act on 319 target genes, among which the metabolites of DM15, DM2, DM17, and DM18 were connected to a greater number of target genes and exhibited the

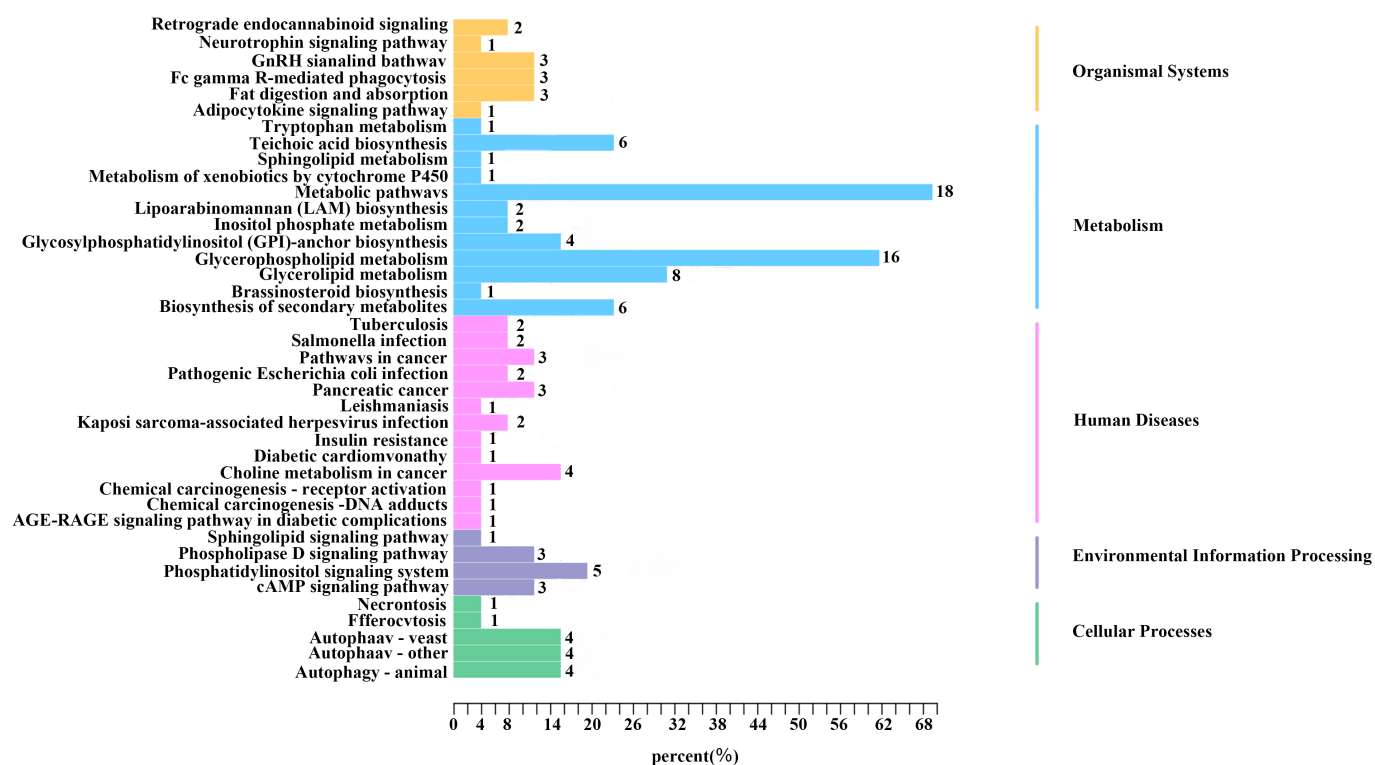


Fig. 5 KEGG enrichment pathway analysis includes environmental information processing channels (10%), cellular processing channels (12.5%), human diseases channels (32.5%), organismal systems channels (15%), and metabolism channels (30%). The numbers following the bars in the figure represent the substances contained in each pathway.

Table 1. The 22 upregulated metabolites and number matching table (DM1–DM22).

Metabolites	Number
16-Methylheptadecanoic acid	DM1
Nonadeca-10(Z)-enoic acid	DM2
11-Eicosenoic acid	DM3
7,7-Dimethyl-(5Z,8Z)-eicosadienoic acid	DM4
2(R)-hydroxydocosanoic acid	DM5
4alpha-Carboxy-5alpha-cholesta-8-en-3beta-ol	DM6
Heliantriol C	DM7
Priverogenin B	DM8
22alpha-Hydroxyerythrodiol	DM9
LysoPC 18:0	DM10
PA 35:3; PA (17:0/18:3)	DM11
PG 32:1; PG (16:0/16:1)	DM12
PG 34:2; PG (16:0/18:2)	DM13
PG 34:2; PG (16:1/18:1)	DM14
8(9)-Epoxy-5Z,11Z,14Z-eicosatrienoic acid, methyl ester	DM15
Betulin	DM16
2-Deoxycasterone	DM17
6-Deoxohomodolichosterone	DM18
1-Stearoyl-2-hydroxy-sn-glycero-3-phosphocholine	DM19
3-cis-Hydroxy-b, e-Caroten-3'-one	DM20
PE (22:4(7Z,10Z,13Z,16Z)/20:5(5Z,8Z,11Z,14Z,17Z))	DM21
DGDG 36:6; DGDG (18:3/18:3)	DM22

highest connectivity. They collectively constituted the key regulatory nodes within the HJFT pharmacological network, suggesting they may play synergistic roles in the regulation of related diseases. Notably, DM18 (6-deoxohomodolichosterone) was identified as having the highest number of predicted target genes, mainly including *PARP1*, *HMGCR*, *NPC1L1*, *PPARG*, *CYP19A1*, *JAK3*, *OPRM1*, *PTGS1*, etc. As a steroidal compound, 6-deoxohomodolichosterone and

its analogues are mainly involved in plant hormone regulation or play physiological roles as secondary metabolites^[19]. It may also have potential anti-inflammatory, immune, or metabolic regulation-related activities^[20], indicating DM18 may have significant potential for disease modulation.

Construction and analysis of the disease-target network

To further predict the physiological functions of HJFT and elucidate the regulatory relationship and synergistic effects between metabolite targets and disease targets, a disease-target network was constructed. The predicted disease keywords for screening in the simulated network were determined based on the main effects and research of FT and Huangjing, including 'anti-oxidant'^[21,22], 'hypertension (HTN)'^[23], 'anti-obesity'^[12,24,25], 'type 2 diabetes mellitus (T2DM)'^[26–28], 'metabolic syndrome (MS)'^[5], and 'tumor (TNM)'^[9,29] to screen the GeneCards database (<https://auth.lifemapsc.com>). The median relevance score was used as the cutoff for the results. Venn diagrams were utilized to visualize the overlap between the predicted targets of 22 upregulated metabolites in HJFT and the predicted target genes associated with the six diseases mentioned earlier. As shown in **Supplementary Fig. S1**, T2DM shared the highest number of overlap genes (101 genes), suggesting the broadest regulatory effects on this condition (**Supplementary Fig. S1d**). In contrast, HTN showed the least number of overlapping genes (32 genes) among the six diseases, reflecting the distinct distributions of disease-specific targets (**Supplementary Fig. S1b**). A multi-set Venn diagram (**Fig. 7a**) was then employed to integrate these intersections and identify potential target genes for the overlap of HJFT metabolites and six diseases. One candidate target gene, *PPARG* (Peroxisome proliferator-activated receptor gamma), common to all six diseases, was identified in the HJFT metabolite (central area, **Fig. 7a**). *PPARG* is one of the three members of the

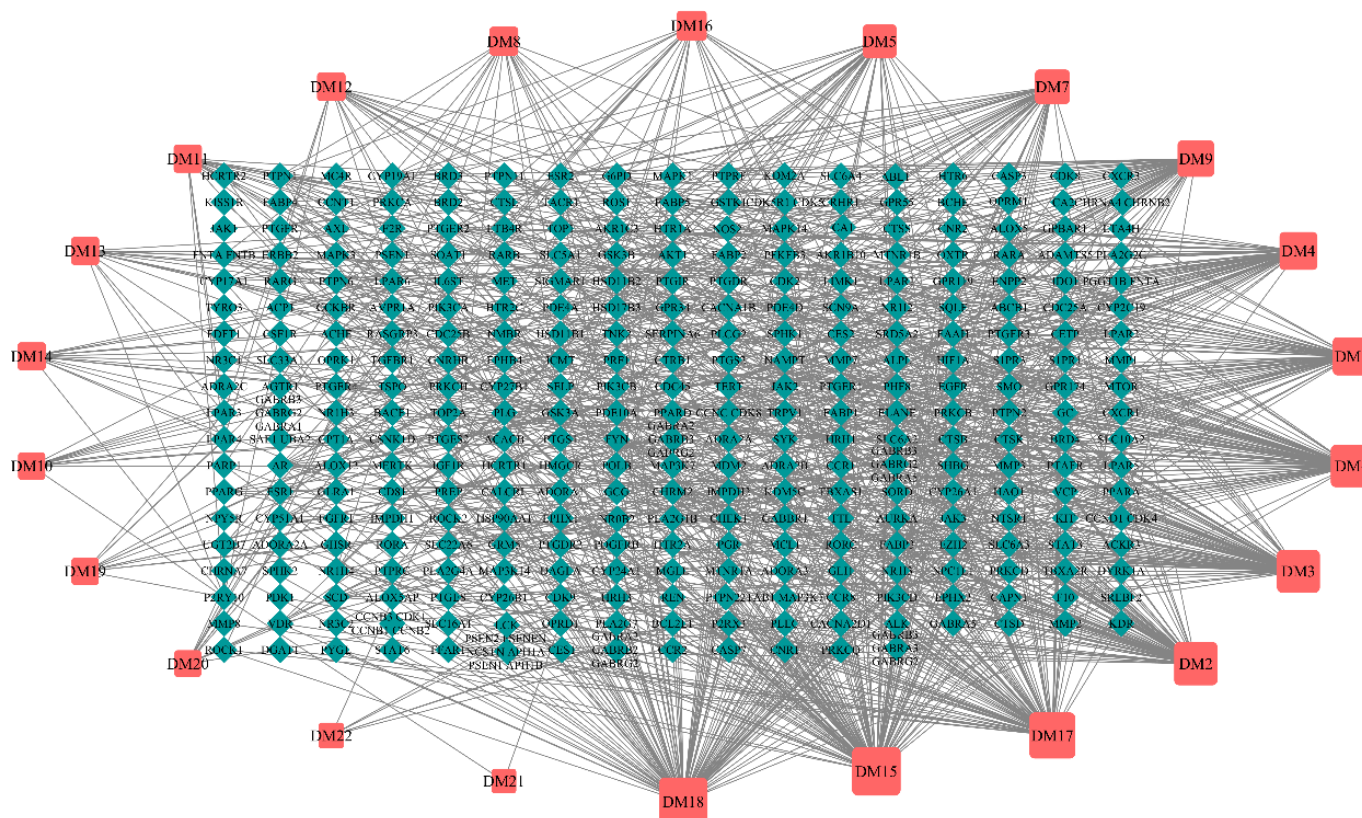


Fig. 6 Metabolite-target network analysis. The red box represents metabolites; the light blue diamond represents the target genes.

PPAR family, which has direct or indirect effects on six different diseases. It is the main gene that could induce the differentiation of adipocytes, enhance insulin sensitivity, regulate adipocyte differentiation, inhibit the cell cycle process, coordinate the systemic anti-inflammatory, and exert anti-oxidant responses, thus regarded as a tumor suppressor factor in oncology^[30,31]. In addition, the shared target genes varied among different diseases. For example, T2DM had nine common target genes with MS, three common target genes with anti-obesity, two common target genes with HTN, and seven common target genes with TNM. These findings indicate that there are complex functional gene networks and potential mechanisms between metabolites in HJFT and diseases.

Furthermore, focusing on the disease-related target genes identified in Fig. 7a, a disease-target association network was developed. As shown in Fig. 7b, a purple oval represents the disease, and the connected target genes were categorized into two types: light blue nodes represent multi-disease (two or more) associated targets, and the remaining nodes represent single disease-specific targets. This network visually demonstrates the commonality and specificity of target genes across the six diseases. For example, T2DM was the disease with the most (101) overlapping screened gene targets.

By intersecting the genes obtained from the six diseases with the genes of the upregulated substances, and then performing a cross-match on the resulting intersection genes, a disease-gene association diagram can be obtained. Violet nodes are for disease, like blue nodes are marked as targets that can act on two or more diseases, while other nodes are targets of a single disease.

Integrated metabolite-target-disease network

Based on an integrated network pharmacology strategy designed to further reveal and predict the synergistic regulatory potential of HJFT metabolites, a global metabolite-target-disease three-layer

interaction network was constructed. This network was established by integrating the metabolite-target network (Fig. 6) with the disease-target networks (Fig. 7). The metabolite nodes were arranged counterclockwise, while the disease nodes were arranged clockwise, both in descending order of node degree value. Following an intersection analysis of the 22 metabolite targets and disease targets, one metabolite was found to have no matching disease genes, and the remaining metabolites and associated diseases were mapped using Cytoscape3.10 to generate the final interaction network (Fig. 8a). The results indicated that specific metabolites, including nonadeca-10(Z)-enoic acid (DM2), 11-eicosenoic acid (DM3), 4 α -carboxy-5 α -cholesta-8-en-3 β -ol (DM6), 2-deoxycastasterone (DM17), 6-deoxohomodolichosterone (DM18), 7,7-dimethyl-(5Z,8Z)-eicosadienoic acid (DM4), 22 α -hydroxyerythrodiol (DM9), 16-methylheptadecanoic acid (DM1), and heliantriol C (DM7) might play a therapeutic role in MS and anti obesity. These effects could be mediated through key target genes, such as *CYP19A1*, *AR*, *PPAR δ* , *FABP4*, and *HMGCR*. Notably, T2DM exhibited the highest degree of overlapping target coverage, suggesting that the prevention and treatment of T2DM could be the most significant activity for HJFT. Therefore, Fig. 8a systematically exhibited the core roles of HJFT metabolites in the disease regulation network of MS and T2DM, providing the evidence and prediction framework for understanding its systemic pharmacological function.

GO function and KEGG pathway enrichment analysis

To further predict the biological function of HJFT metabolites, GO enrichment and KEGG pathway^[32] enrichment analyses were performed using the targets of 22 upregulated metabolites through Metascape (<http://metascape.org>)^[17]. The top 10 pathways with the highest proportion and the lowest *p*-values were analyzed, with the top five classes displayed (Fig 8b). The target genes were

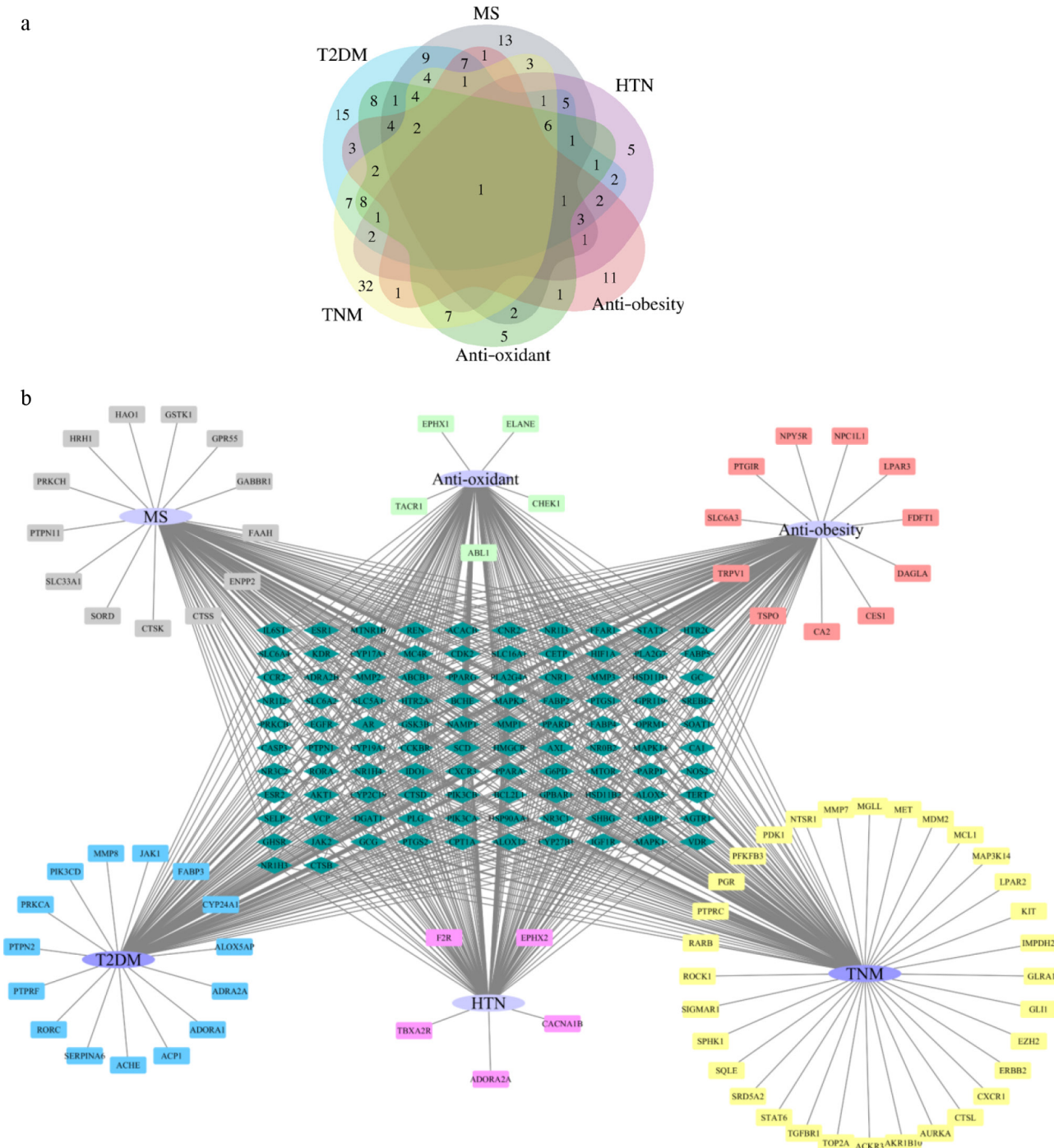


Fig. 7 Disease-target diagram. (a) The Venn diagram comprehensive overlap of up-regulate metabolite-target and six types of disease-targets; (b) Six types of disease targets network (Purple nodes represent the diseases, light blue nodes represent multi disease associated targets, which associated with two or more diseases, the highlighted rectangles represent disease-specific targets, which linked to a single disease).

significantly enriched in signaling pathways such as neuroactive ligand-receptor interactions, pathways in cancer, MAPK signaling pathways, as well as others related to inflammatory immunity and anti-atherosclerosis (e.g., EGFR tyrosine kinase inhibitor resistance, inflammatory mediator regulation of TRP channels, PPAR signaling pathway, etc.). In terms of BP, the target genes were mainly enriched in cellular responses to hormone stimulus; regulation of hormone levels, system processes, MAPK cascades, and positive regulation of locomotion for biological processes. CC were primarily enriched in

receptor complexes, postsynapse, the side of the membrane, the neuronal cell body, and the membrane raft. The stimulating target genes were enriched in MF, including enzyme activity of various types, receptor activity, and compound binding. Network pharmacology simulation analysis demonstrated the multi-target, multi-pathway, and multi-functional characteristics of the main upregulated metabolites from HJFT, which may play a potential functional role in regulating neurotransmitter receptor activity, diabetes, the immune system, and vascular function.

The metabolites and physiological activity of HJFT

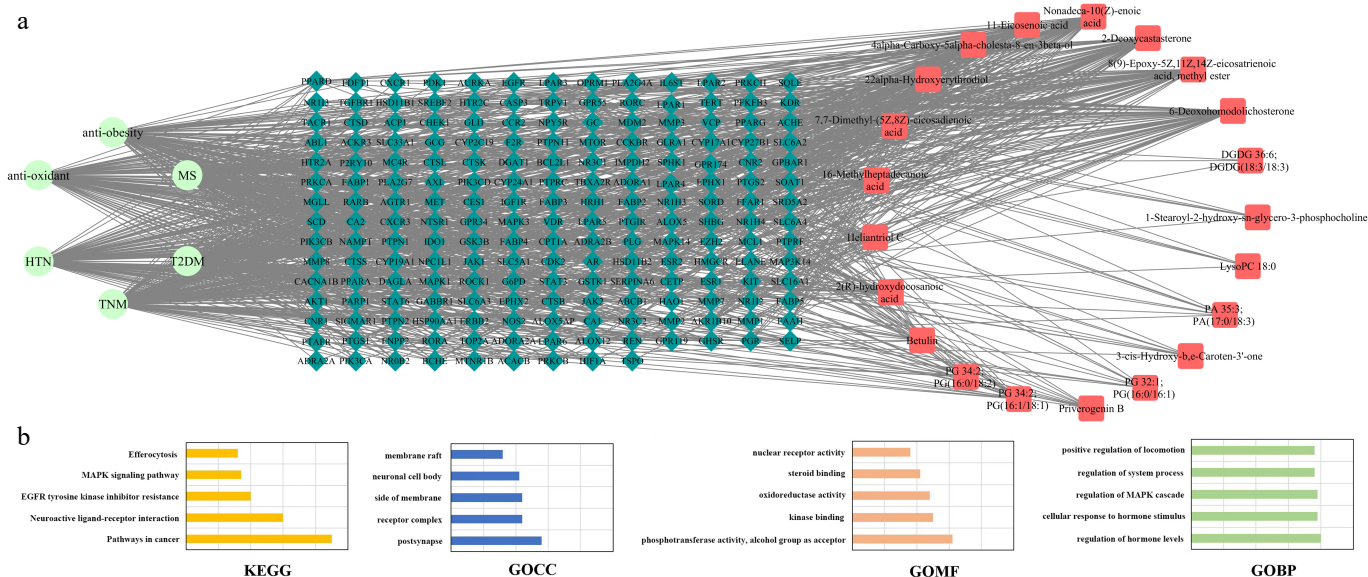


Fig. 8 Disease-target-metabolite analysis diagram. (a) Disease-target-metabolite pharmacology network. (The green nodes represent diseases, the red nodes represent metabolites, and the lake blue nodes represent target genes with common interaction associations. Node size represents the degree value). (b) The top five pathways of disease-target-metabolite enrichment. (From top to bottom: KEGG pathway enrichment, GOCC pathway enrichment, GOMF pathway enrichment, and GOBP pathway enrichment).

Discussion

This study analyzed the differential metabolites of HJFT and FT, and found that the lipid class, including MGDG, DGDG, and PA linked to aroma formation were significantly increased in HJFT. Elevated DGDG and PA indicated oxidative degradation during the 'flowering' process. At the same time, the increase of AcylGlcADG, presented as a key lipid in probiotic outer vesicles, significantly promoted the growth of *E. cristatum* during the 'flowering' process. Besides, an increase in the content of sterols (2-deoxycasterone, 6-deoxohomodolichosterone) was found, which are normally used in clinical prevention and treatment of coronary artery atherosclerosis and other heart diseases^[33], with anti-inflammatory, cholesterolregulatory, and cardiovascular protective effects on the human body^[34]. Furthermore, among the differential metabolites, 3-cis-Hydroxy-b, and e-Caroten-3'-one, a class of carotene derivative, was found to be one of the characteristic products of the metabolic transformation of carotenoids in FT by *E. cristatum*^[35,36]. It was actually formed by the degradation of carotenoids during the flowering process, together with a water-soluble colored product formed by the partial oxidation and polymerization of tea polyphenols. The two products reacted with unoxidized amino acids and flavonoids, and finally formed the typical leaf color and orange-yellow soup color of Fu tea^[34]. In addition, betulin and priverogenin B, both belonging to the terpene/steroid substance group, as well as steroid saponins, the core active component of Huangjing, were increased probably because of the addition of Huangjing^[11,16]. These substances have been proven to have certain pharmacological activities in anti-inflammation, virus inhibition, anti-aging, and oxidation (especially in skin repair)^[8,37].

Obesity and metabolic disease, hypertension, and T2DM have gradually emerged as major global public health issues^[38]. Huangjing and FT, respectively, have pharmacological effects^[5,12,24,39,40] against such diseases. In this study, network pharmacology identified T2DM as the disease with the highest number of overlapping gene targets, indicating HJFT may have a potential function in anti-diabetic prevention or treatment. According to the

analysis results on the key pathways, including MAPK, AGE-RAGE (diabetic complications), GnRH, and cAMP signaling (anti-diabetic), the activation of the AGE-RAGE signaling pathway was particularly noteworthy, as the tocotrienol fraction in palm oil has been proven to be able to improve plasma redox imbalance and AGE-RAGE activation in high-fat diet rats^[41]. Other related pathways, including glycerolipid, glycerophospholipid metabolism, and secondary metabolite, which mostly cover the degradation of phospholipids (such as PG, PE, etc.), and the hydrolysis and oxidation of glycerides (such as MGDG, DGDG, etc.), contributed to the Fu tea characteristic mushroom flavour^[35,42,43]. The enriched pathways, including brassinosteroid biosynthesis, glycosylphosphatidylinositol (GPI)-anchor biosynthesis, fat digestion and absorption, and insulin resistance, were generally considered to be associated with the treatment of obesity and diabetes^[44], and the efficiency has been verified in multiple studies in which T2DM in obese mice was treated with Fu brick tea^[26]. The main mechanism of obesity alleviation^[40] was by remodeling gut microbiota and regulating gut metabolites^[5,24,26]. *Polygonatum sibiricum* polysaccharide (PSP) has been confirmed to exert anti-aging effects through the sphingolipid signaling pathway^[45], glycerophospholipid and tryptophan metabolism, as well as modulating diabetic osteoporosis via sphingolipid signaling^[46]. Other metabolic pathways related to human diseases include Kaposi sarcoma-associated herpes virus infections, pathways in cancer, Salmonella infection, leishmaniasis, choline metabolism in cancer, tuberculosis, and pathogenic *Escherichia coli* infection.

Currently, Huangjing composites have been widely applied in wines^[14], beverages, cosmetics, and feeds^[10]. Compared to FT, HJFT demonstrates richer processing-related substance metabolism, thereby enhancing the aroma and flavor of the tea, as well as the biological and pharmacological activities. However, in this study, the pharmacological properties of HJFT were predicted solely through simulation calculations and analysis; the utilization rate of active compounds in HJFT remains limited. In the future, it is necessary to validate these specific functional bioactive metabolites and conduct

relevant *in vivo* and *in vitro* experiments to verify their efficacy in order to promote the application of innovative Fu tea products and HJFT in the beverage and health fields.

Conclusions

A total of 49 different metabolites were identified based on the UHPLC-Q-TOF-MS/MS and non-targeted metabolomics analysis. These metabolites were primarily classified into six categories, mainly including lipids and lipid-like molecules, organ heterocyclic compounds, and organic oxygen compounds. Meanwhile, Class II was divided into 12 categories, mainly containing glycerophospholipids, fatty acyls, sterol lipids, organooxygen compounds, and sphingolipidoses. Compared to FT, lipid components such as MGDG, DGDG, and PA were significantly enhanced in HJFT. Meanwhile, HJFT was rich in sterols such as 6-deoxohomodolichosterone and terpenoid derivatives. The integrated network pharmacology analysis predictively indicated that sterols and terpenoid derivatives, which were upregulated in HJFT, exerted effectiveness in hypertension control, T2DM treatment, anti-inflammatory, and anti-oxidant activities primarily via the AGE-RAGE and MAPK signaling pathways. Notably, these metabolites exhibited the most overlapping targets for T2DM, predicting their most prominent potential efficacy in T2DM. These findings elucidate the potential physiological activities of HJFT and lay a scientific basis for its further development and utilization, which may offer valuable references and guidance for the development of similar beverages with dual medicinal and dietary properties.

Author contributions

The authors confirm contribution to the paper as follows: experiments performed: Ma Z, Gu B, Zhang P; data analysis: Ma Z, Zhang M, Gu B, Li C, An C, Zhang P; draft manuscript preparation: Ma Z, Meng Y, An C, Gao Y; study conception and design supervision: An C, Xiao X, Mi L, Gao Y. All authors reviewed the results and approved the final version of the manuscript.

Data availability

All data generated or analyzed during this study are included in this published article and its supplementary information files.

Acknowledgments

This study was supported by the Key Research and Development Program of Shaanxi Province (2025NC-YBXM-143), the Technical Service Projects (24H0819), the Scientific and Technological Innovation Support Plan of Xianyang City (L2023-CXNL-CXRC-008), the Local Government Cooperation Project of Jingyang County (K4050122051), the Youth Foundation of Hebei Education Department (QN2025120) and the Chengde Medical University Project (202404).

Conflict of interest

The authors declare that they have no conflict of interest.

Supplementary information accompanies this paper online at: <https://doi.org/10.48130/bpr-0026-0017>.

Dates

Received 9 February 2026; Revised 6 April 2026; Accepted 20 April 2026; Published online 26 June 2026

References

- [1] Wang Z, Jin Q, Jiang R, Liu Y, Xie H, et al. 2024. Characteristic volatiles of Fu brick tea formed primarily by extracellular enzymes during *Aspergillus cristatus* fermentation. *Food Research International* 177:113854
- [2] Xiao Y, Zhong K, Bai JR, Wu YP, Gao H. 2020. Insight into effects of isolated *Eurotium cristatum* from Pingwu Fuzhuan brick tea on the fermentation process and quality characteristics of Fuzhuan brick tea. *Journal of the Science of Food and Agriculture* 100(9):3598–3607
- [3] Wu H, Zhao H, Ding J, Wang Y, Hou J, et al. 2023. Metabolites and microbial characteristics of Fu brick tea after natural fermentation. *LWT* 181:114775
- [4] Zhao R, Yao H, Hou Z, Zhou Q, Zhao M, et al. 2024. Sensomics-assisted analysis unravels the formation of the Fungus Aroma of Fu Brick Tea. *Food Chemistry* 458:140174
- [5] Li H, Dai W, Zhang X, Lu J, Song F, et al. 2024. Chemical components of Fu brick tea and its potential preventive effects on metabolic syndrome. *Food Science & Nutrition* 12(1):35–47
- [6] Yang M, Zhou L, Kan Z, Fu Z, Zhang X, et al. 2025. Beneficial health effects and possible health concerns of tea consumption: a review. *Beverage Plant Research* 5:e035
- [7] Yang M, Chen R, Zhou X, Chen H. 2024. Research progress on pharmacological effects and mechanism of *Polygonatum sibiricum* polysaccharides. *Starch – Stärke* 76(9–10):2300168
- [8] Zhao X, Patil S, Qian A, Zhao C. 2022. Bioactive compounds of *Polygonatum sibiricum* – therapeutic effect and biological activity. *Endocrine, Metabolic & Immune Disorders – Drug Targets* 22(1):26–37
- [9] Zhu M, Chen G, Li J, Yi C, Yuan Y, et al. 2025. The antitumor potential of *Polygonatum* spp. : a narrative review of traditional uses, bioactive metabolites, and multi-targeted mechanisms. *Frontiers in Pharmacology* 16:1662839
- [10] Li P, Yao H, Yue H, Huang J, Wang Q, et al. 2025. Preparation, structure, function, and application of dietary polysaccharides from *Polygonatum sibiricum* in the food industry: a review. *Molecules* 30(5):1098
- [11] Liu R, Zhang X, Cai Y, Xu S, Xu Q, et al. 2024. Research progress on medicinal components and pharmacological activities of *Polygonatum sibiricum*. *Journal of Ethnopharmacology* 328:118024
- [12] Guo Q, Yuan J, Ding S, Nie Q, Xu Q, et al. 2024. Microbial fermentation in fermented tea beverages: transforming flavor and enhancing bioactivity. *Beverage Plant Research* 4:e029
- [13] Ou X, Wang X, Zhao B, Zhao Y, Liu H, et al. 2023. Metabolome and transcriptome signatures shed light on the anti-obesity effect of *Polygonatum sibiricum*. *Frontiers in Plant Science* 14:1181861
- [14] Wang JJ, Zhang WW, Guan ZJ, Thakur K, Hu F, et al. 2023. Exploring the effects of the fermentation method on the quality of *Lycium barbarum* and *Polygonatum cyrtonea* compound wine based on LC-MS metabolomics. *Food Chemistry* 428:136770
- [15] Zhang JG, Wang JJ, Zhang WW, Guan ZJ, Thakur K, et al. 2024. Metabolomics and HS-SPME-GC-MS-based analysis of quality succession patterns and flavor characteristics changes during the fermentation of *Lycium barbarum* and *Polygonatum cyrtonea* compound wine. *Food Research International* 184:114270
- [16] Sun Y, Zhou L, Shan X, Zhao T, Cui M, et al. 2023. Untargeted components and *in vivo* metabolites analyses of *Polygonatum* under different processing times. *LWT* 173:114334
- [17] Zhou Y, Zhou B, Pache L, Chang M, Khodabakhshi AH, et al. 2019. Metascape provides a biologist-oriented resource for the analysis of systems-level datasets. *Nature Communications* 10:1523
- [18] Kanehisa M, Furumichi M, Sato Y, Matsuura Y, Ishiguro-Watanabe M. 2025. KEGG: biological systems database as a model of the real world. *Nucleic Acids Research* 53(D1):D672–D677

- [19] Takatsuto S, Ikekawa N. 1986. Synthesis of 6-deoxohomodolichosterone, a new plant-growth-promoting steroid. *Journal of the Chemical Society, Perkin Transactions 1*:2269
- [20] Liu F, Li L, Tian X, Zhang D, Sun W, et al. 2021. Chemical constituents and pharmacological activities of steroid saponins isolated from rhizoma paridis. *Journal of Chemistry* 2021(1):1442906
- [21] Tan Z, Yu P, Zhu H, Gao J, Han N, et al. 2024. Differential characteristics of chemical composition, fermentation metabolites and antioxidant effects of polysaccharides from *Eurotium cristatum* and Fu-brick tea. *Food Chemistry* 461:140934
- [22] Li L, Thakur K, Liao BY, Zhang JG, Wei ZJ. 2018. Antioxidant and antimicrobial potential of polysaccharides sequentially extracted from *Polygonatum cyrtoneuma* Hua. *International Journal of Biological Macromolecules* 114:317–323
- [23] Liu MY, He T, Wang XP, Feng H, Li XF, et al. 2024. Based on LC–MS and network pharmacology, the quality components, and anti-hypertensive mechanisms of three types of tea were studied. *Journal of Food Science* 89(12):8276–8295
- [24] Du H, Shi L, Yan T, Wang Q, Wang Y, et al. 2022. Fu brick tea protects against high-fat diet-induced obesity phenotypes via promoting adipose browning and thermogenesis in association with gut microbiota. *Food & Function* 13(21):11111–11124
- [25] Alawiyah YS, Rimbawan R, Dewi M. 2025. The effect of green tea and *Moringa oleifera* tea brewing on lipid profiles in overweight and obese subject: a clinical trial. *Beverage Plant Research* 5:e039
- [26] Qi B, Ren D, Li T, Niu P, Zhang X, et al. 2022. Fu brick tea manages HFD/STZ-induced type 2 diabetes by regulating the gut microbiota and activating the IRS1/PI3K/Akt signaling pathway. *Journal of Agricultural and Food Chemistry* 70(27):8274–8287
- [27] Wang G, Liu Z, Liang D, Yu J, Wang T, et al. 2022. Aqueous extract of *Polygonatum sibiricum* ameliorates glucose and lipid metabolism via PI3K/AKT signaling pathway in high-fat diet and streptozotocin-induced diabetic mice. *Journal of Food Biochemistry* 46(12):e14402
- [28] Zhao L, Lin J, Li L, Ge ZJ. 2025. Benefits of tea on the reproductive health of diabetes mellitus. *Beverage Plant Research* 5:e019
- [29] Chen J, Xia J, Yin F, Yu J, Huo J, et al. 2023. UPLC-Q-exactive-MS combined with network pharmacology to explore the antitumor effect of *Polygonatum sibiricum* leaf tea. *Journal of Food Biochemistry* 2023(1):4174625
- [30] Majithia AR, Flannick J, Shahinian P, Guo M, Bray MA, et al. 2014. Rare variants in *PPARG* with decreased activity in adipocyte differentiation are associated with increased risk of type 2 diabetes. *Proceedings of the National Academy of Sciences of the United States of America* 111(36):13127–13132
- [31] Siersbæk R, Nielsen R, Mandrup S. 2010. *PPAR γ* in adipocyte differentiation and metabolism—Novel insights from genome-wide studies. *FEBS Letters* 584(15):3242–3249
- [32] Kanehisa M. 2019. Toward understanding the origin and evolution of cellular organisms. *Protein Science* 28(11):1947–1951
- [33] Ye Y, Xia C, Hu H, Tang S, Huan H. 2024. Metabolomics reveals altered metabolites in cirrhotic patients with severe portal hypertension in Tibetan population. *Frontiers in Medicine* 11:1404442
- [34] Liu S, Jiao W, Ni H, Ren F, Wang Y. 2026. Natural phytosterols as the nutraceuticals or functional agents: insights into structure–activity relationship. *Comprehensive Reviews in Food Science and Food Safety* 25(1):e70359
- [35] Xiao Y, He C, Chen Y, Ho CT, Wu X, et al. 2022. UPLC–QQQ–MS/MS-based widely targeted metabolomic analysis reveals the effect of solid-state fermentation with *Eurotium cristatum* on the dynamic changes in the metabolite profile of dark tea. *Food Chemistry* 378:131999
- [36] Liu W, Shen J, Luo X, Lv X, Liu Z, et al. 2025. Beyond pigmentation: the regulatory role of carotenoids in tea flavor formation. *Comprehensive Reviews in Food Science and Food Safety* 24(5):e70284
- [37] Hu Y, Yin M, Bai Y, Chu S, Zhang L, et al. 2022. An evaluation of traits, nutritional, and medicinal component quality of *Polygonatum cyrtoneuma* Hua and *P. sibiricum* red. *Frontiers in Plant Science* 13:891775
- [38] Li J, Zhou Y, Tang Y, Liu Z, Zhang S, et al. 2025. Effect of pu-erh tea compound solid beverage on weight loss of high-fat diet mice. *Beverage Plant Research* 5:e014
- [39] Wang H, Fowler MI, Messenger DJ, Terry LA, Gu X, et al. 2018. Homoisoflavonoids are potent glucose transporter 2 (GLUT2) inhibitors: a potential mechanism for the glucose-lowering properties of *Polygonatum odoratum*. *Journal of Agricultural and Food Chemistry* 66(12):3137–3145
- [40] Jian OY, Li XP, Liu CW, Jie OY, Tang JY, et al. 2023. Moringa-Fu brick tea extract attenuated high-fat diet-induced obesity via modulating bile acid metabolism and gut microbiota in rats. *Journal of Functional Foods* 109:105766
- [41] Cheng H, Ton S, Tan J, Abdul Kadir K. 2017. The ameliorative effects of a tocotrienol-rich fraction on the AGE-RAGE axis and hypertension in high-fat-diet-fed rats with metabolic syndrome. *Nutrients* 9(9):984
- [42] Chen L, Ma J, Niu L, Feng Y, Fang Z, et al. 2025. Lipid profiles and metabolic characteristics of Chinese tea cultivars (*Camellia sinensis*) with different manufacturing suitabilities by comparative lipidomics using UHPLC-Q-Exactive mass spectrometry. *Food Chemistry* 488:144882
- [43] Xiao Y, Huang Y, Chen Y, Zhu M, He C, et al. 2022. Characteristic fingerprints and change of volatile organic compounds of dark teas during solid-state fermentation with *Eurotium cristatum* by using HS-GC-IMS, HS-SPME-GC-MS, E-nose and sensory evaluation. *LWT* 169:113925
- [44] Huang X, Liu G, Guo J, Su Z. 2018. The PI3K/AKT pathway in obesity and type 2 diabetes. *International Journal of Biological Sciences* 14(11):1483–1496
- [45] Shen D, Feng Y, Zhang X, Gong L, Liu J, et al. 2022. Antiosteoporosis studies of 20 medicine food homology plants containing quercetin, rutin, and kaempferol: TCM characteristics, *in vivo* and *in vitro* activities, potential mechanisms, and food functions. *Evidence-Based Complementary and Alternative Medicine* 2022(1):5902293
- [46] Ren Y, Sun Y, Liao YY, Wang S, Liu Q, et al. 2024. Mechanisms of action and applications of *Polygonatum sibiricum* polysaccharide at the intestinal mucosa barrier: a review. *Frontiers in Pharmacology* 15:1421607



Copyright: © 2026 by the author(s). Published by Maximum Academic Press, Fayetteville, GA. This article is an open access article distributed under Creative Commons Attribution License (CC BY 4.0), visit <https://creativecommons.org/licenses/by/4.0/>.